Eur. Phys. J. B **15**, 21–27 (2000)

THE EUROPEAN PHYSICAL JOURNAL B

EDP Sciences

Spin density distribution of the conduction electrons in diperylene hexafluorophosphate analysed by high-resolution NMR

G. Fischer[1,a] and E. Dormann[1]

Physikalisches Institut, Universität Karlsruhe (TH), 76128 Karlsruhe, Germany

Received 29 June 1999 and Received in final form 4 November 1999

Abstract. High-resolution ^{13}C nuclear magnetic resonance with ^{1}H cross polarization and ^{1}H decoupling under magic angle spinning is measured for the quasi-one dimensional organic conductor diperylene hexafluorophosphate (including tetrahydrofurane solvent molecules) at temperatures between 160 K and 270 K. *Ab initio* molecular orbital calculations are used for chemical shift analysis and for assignment of Knight shifted lines and individual carbon positions. The coexistence of neutral perylene molecules and perylene radicals in the same radical cation salt is revealed. From Knight and chemical shifts we were able to distinguish two inequivalent perylene radicals within the conducting stack. The spin density distribution of the molecular electronic wave function is determined quantitatively for these radicals.

PACS. 76.60.Cq Chemical and Knight shifts – 71.20.-b Electron density of states and band structure of crystalline solids

1 Introduction

Diperylene hexafluorophosphate is an especially interesting quasi-one dimensional organic conductor [1,2]. In contrast to the first supposition suggested by the composition $(PE)_2PF_6 \cdot \frac{2}{3}THF$ (with PE: perylene, THF: tetrahydrofurane), this organic conductor has not a three-quarter filled conduction band as the majority of other radical cation salts (RCS) with 2:1 stoichiometry. The band filling amounts to five eights in the extended band scheme, and the properties of this RCS are more closely described by the formula $(PE)_4^{3+\bullet\bullet\bullet}(PE)_2^0(PF_6^-)_3 \cdot 2\,THF$ [3]. Four PE radicals with an average charge of $+3/4\,e$ form the elementary unit of the one-dimensional conducting stack. They are surrounded by neutral PE molecules, PF_6^- anions and partially disordered THF solvent molecules forming the "walls" of the conducting channels (see Fig. 1).

Below the Peierls transition at $T_p = 118$ K, superstructure X-ray reflections reveal a doubling of the unit cell in stacking direction c. Thus eight PE radicals form the repetition unit which gives rise to the gap in the electronic density of states at the Fermi energy. Already at higher temperatures the crystal symmetry is reduced from monoclinic to triclinic at $T_t = 213$ K and subsequently at $T_r = 153$ K, the unit cell is doubled in the crystallographic a direction, accompanied with the slowing down of the THF-solvent and the PF_6^--molecules rotational motion [4–6]. Quite a number of experimental techniques were combined in order to deduce a conclusive picture of electronic and structural properties of the $(PE)_2PF_6 \cdot \frac{2}{3}THF$ salts. The most fundamental information is obtained from high-resolution ^{13}C-NMR [7], as will be presented below. This NMR analysis allows to separate the signals of neutral from charged PE molecules coexisting within this RCS. Two inequivalent sites of charged PE molecules in the quasi-one dimensional PE stack can be resolved which gives access to the local spin densities at the carbon sites of the PE radicals *via* quantitative analysis of the different temperature-dependent Knight shifts. Preliminary results have been reported elsewhere [8,9].

This report is organized as follows: the NMR techniques adopted are described in Section 2. Our analysis is restricted to temperatures above T_r, *i.e.*, to the monoclinic and triclinic phase (preventing doubling of the unit cell along the a direction). The derivation of the molecular electronic wave function *via* the quantitative analysis of the locally resolved isotropic part of the Knight shifts requires the separation of Knight and chemical shifts. The chemical shifts for the different ^{13}C nuclei in neutral PE molecules are determined experimentally and *via* model calculations (Sect. 3.1). Details of the experimental derivation of the locally resolved Knight shifts are reported in Section 3.2. The determination of the local spin densities at the carbon sites C1-C6 (see Fig. 1c) of the PE radical is discussed in Section 3.3, followed by concluding remarks in Section 4.

2 Experimental details

Small needle like crystals of $(PE)_2PF_6 \cdot \frac{2}{3}THF$ were grown electrochemically as described elsewhere [2].

[a] e-mail: Gerda.Fischer@physik.uni-karlsruhe.de

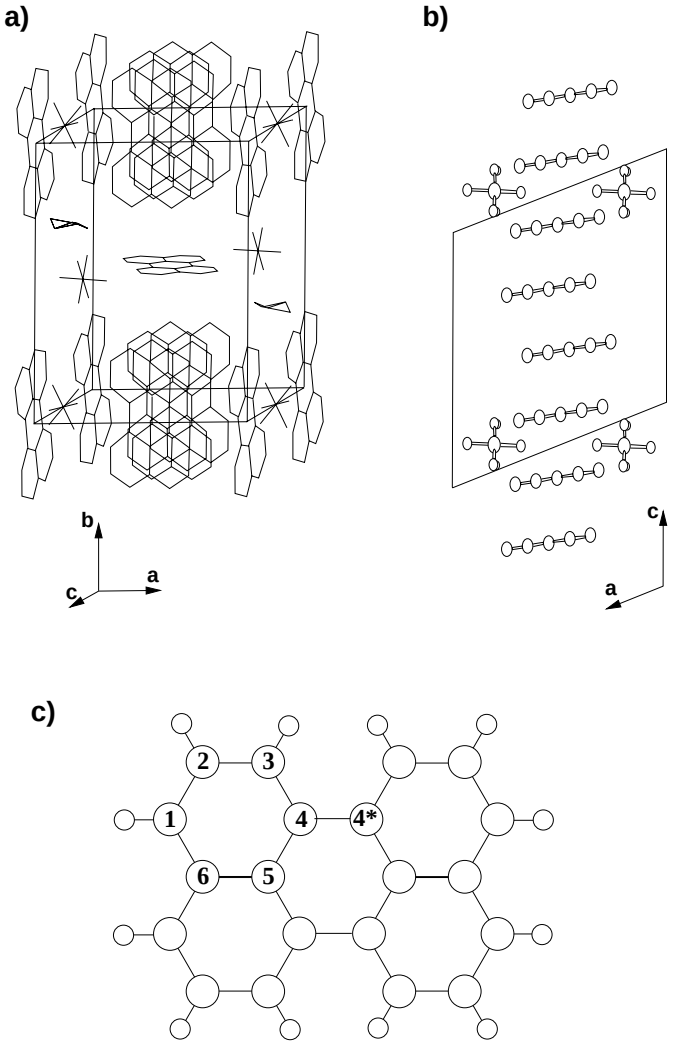

Fig. 1. (a) Crystal structure of $(PE)_2PF_6 \cdot \frac{2}{3}THF$ [2] seen along the stacking axis *c*. (b) View along *b* showing the PE stack. (c) Schematic presentation of a perylene molecule ($C_{20}H_{12}$) with numbering of the C atoms as used in the text.

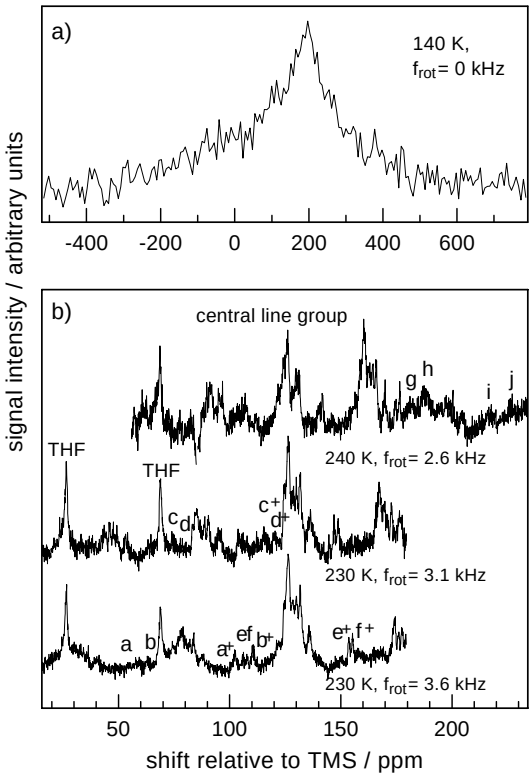

Fig. 2. ^{13}C spectra of diperylene hexafluorophosphate. (a) Normal resolution. (b) High-resolution achieved by ^{13}C-CP-MAS showing all determined resonance lines.

The measurements were performed with a Bruker MSL-300 spectrometer operating at a frequency of 75.468 MHz for ^{13}C and 300.13 MHz for ^{1}H. High-resolution for natural abundance of ^{13}C was achieved by sample spinning at the magic angle, cross polarisation between ^{1}H and ^{13}C, and proton decoupling. Samples consisting of statistically oriented single crystals were used. We did not powder the samples [10,11], accepting an associated loss of resolution. This was done in order to prevent the formation of paramagnetic defects, which are induced by breaking the solvent-including crystals and thus increasing the defect concentration above 10^{-3}. The contact time for polarisation transfer was between 2 ms and 4 ms. Up to 2500 scans, with a waiting period after each scan of 5 s up to 10 s, gave a reasonable signal intensity for a sample of about 100 mg. The usual gated decoupling technique was employed to identify resonance lines originating from carbons which are directly bound to protons [12,13]. The highest evolution time being 1000 μs. The ^{1}H pulse length and the Hartman-Hahn condition were adjusted using the test substance Adamantane. Nitrogen gas from evaporation of liquid nitrogen was used both for spinning and cooling the sample. The temperature range was between 160 K (limited by the pre-cooled nitrogen gas) and 270 K (due to the restricted stability of the crystals at higher temperatures). The line width of the normally resolved ^{13}C powder spectrum of perylene in the perylene radical cation salt is about 12 kHz (Fig. 2a). This exceeds the highest spinning frequency of $f_{\rm rot} = 4.5$ kHz useful in this analysis due to eddy current braking, sample size and weight. Therefore careful analysis for the high-resolution spectra (Fig. 2b) was necessary to distinguish real lines from spinning side bands appearing symmetrically on both sides of the real lines in multiples of the spinning frequency.

The chemical shift for pure perylene is given relative to tetramethylsilane (TMS) *via* adamantane as secondary reference within the sample. Adamantane shows two lines, $A_1 = 29.5$ ppm and $A_2 = 38.5$ ppm, which are known from the literature [14]. Unfortunately, parts of the spectrum of $(PE)_2PF_6 \cdot \frac{2}{3}THF$ are superimposed by the adamantane lines. The signal of the solvent THF, which is incorporated within the crystals, proved to be strong enough as secondary reference, however. The two line positions relative to TMS have been measured as $THF_1 = 26.1$ ppm and $THF_2 = 67.9$ ppm (also seen in Fig. 2b).

3 Discussion of the results

3.1 Reference for chemical and Knight shift

The chemical shift of molecules in a conducting material is usually taken to be the same as the chemical shift in the neutral constituent. This chemical shift is also used as reference for the Knight shift in the conducting material [15].

Therefore, the ^{13}C-CP-MAS spectrum of pure neutral perylene has been measured (open symbols in Fig. 3). It consists -typically for an aromatic material- of several lines between 115 ppm and 140 ppm with the center of gravity being at 127.2 ppm. A complete line assignment is carried out in three steps. First, the area under the spectrum is fitted by the superposition of ten Gaussian lines which have all the same area (solid line in Fig. 3). These ten lines stand for the six different carbon positions on the perylene molecule, four of which occur twice as often as the other two positions (see Fig. 1c). Thus positions with double intensity (C1 to C4) and single intensity (C5 or C6) can be distinguished. There is only one uncertainty, because one Gaussian line with single intensity has two possible positions (first two columns of Tab. 1). In a second step, the chemical shift for the different carbon positions on the perylene molecule are calculated with help of the package MPSHIFT of the program TURBOMOLE [16]. In these molecular orbital (MO) calculations the relative position of the chemical shifts of different carbon atoms appear to be more accurate then their absolute position. Therefore, in the third step, Gaussian lines with the normalised area from the area-fit are placed at these calculated positions to form a spectrum (dotted line in Fig. 3). By comparison of this constructed spectrum with the measurement the peaks in the spectrum of pure perylene can be assigned to the different carbon positions on the perylene molecule (Fig. 3, Tab. 1).

With this result, the chemical shift of a pure neutral perylene, either the center of gravity of the spectrum or the individual shifts δ_i of different carbon positions, can be used as a reference for the Knight shift K_i of the different carbon positions in the perylene RCS. In the temperature range above T_t with no structural transitions the chemical shift, which is very sensitive to the geometry of a molecule, is independent of temperature. For temperature independent hyperfine coupling constants a_i the Knight shift has the same temperature variation as the susceptibility of the conduction electrons:

$$K_i = a_i \, \chi_{ce}(T)/(g_e \, \mu_B \, {}^{13}\gamma \, \hbar). \qquad (1)$$

As will be seen below, the monoclinic to triclinic structural transition can be seen in the shift $(K_i + \delta_i)$ *versus* T or in dependence of $\chi_{ce}(T)$, however.

3.2 High-resolution spectra of $(PE)_2PF_6 \cdot \frac{2}{3}THF$

Complete high-resolution spectra of $(PE)_2PF_6 \cdot \frac{2}{3}THF$ measured at about 230 K are shown in Figure 2b. They are dominated by a group of resonance lines between 120 ppm and 140 ppm (further called: central line group) consisting of at least 7 different lines very close to each other. Their center of gravity is at 128.8 ppm. The spinning sidebands of this central line group are not marked. Apart from these there are 10 smaller resonance lines – labeled a to j (with spinning sidebands a^+ to f^+) – spreading from about 50 ppm to 230 ppm. To present all the positions of these real lines the spectrum has to be measured at different spinning frequencies. Otherwise real lines are hidden under spinning side bands of the central line group.

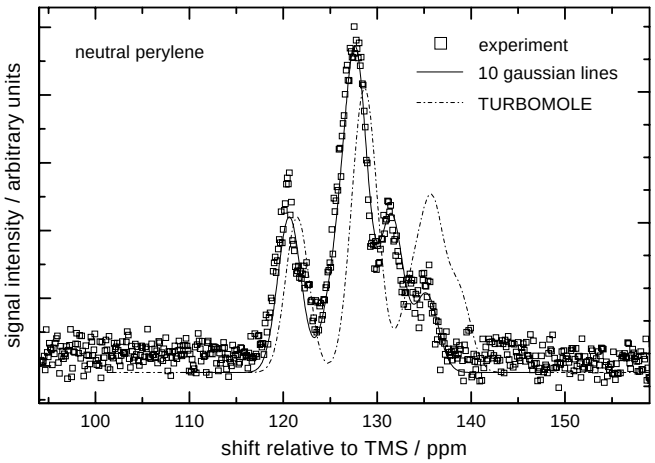

Fig. 3. Measured, fitted, and calculated high-resolution ^{13}C spectra of neutral perylene. For details see text, and the parameters are given in Table 1.

Table 1. Chemical shifts of pure perylene. The first two columns give the results of a fit to the area of the spectrum. The last two columns are the results of the calculations by TURBOMOLE. Therefore a complete line assignment is possible. The last row gives the center of gravity for the measurement and the constructed (see text) spectrum.

atom	$\delta_{i,\mathrm{exp}}$(ppm)	position	$\delta_{i,\mathrm{cal}}$(ppm)
C1-C4	120.6	C3	121.5
C1-C4	127.7	C2	128.1
C1-C4	127.7	C1	129.2
C1-C4	131.5	C4	135.9
C5/C6	125.4/130.0	C5	133.7
C5/C6	135.2	C6	138.7
$\overline{\mathrm{C}}_{\mathrm{exp}}$	127.2	$\overline{\mathrm{C}}_{\mathrm{cal}}$	130.2

3.2.1 The central line group: chemically shifted lines

In Figure 4a we have the spectrum in the range of the central line group. At a constant spinning frequency of 3.7 kHz the temperature is varied from 170 K to 250 K. The positions of these peaks relative to TMS are shown *versus* temperature in Figure 4b. Over the whole temperature range observed the center of gravity (open rhombs)

is stable at 128.8 ppm (mean value given by solid line in Fig. 4b). This is almost the same position as that of pure neutral perylene (127.2 ppm). Because of this close vicinity and the fact that there is no shift with temperature the central line group must be merely chemically shifted. This means that these lines are the resonance signals of neutral perylene molecules within the radical cation salt. They can be assigned to the perylene wall molecules within the crystal structure (Fig. 1). This is therefore the first explicit experimental proof that these molecules in the RCS are neutral and do not participate in the charge transfer to the anions.

Although the center of gravity is within the experimental error the same over the whole temperature range, there is a shift of intensity between 220 K and 190 K within the central line group. Figure 4 shows that there is a rearrangement of intensity within the central line group from peak 3 to peak 4. This is probably due to the above mentioned structural phase transition at $T_t = 213$ K and the sensitivity of the chemical shift to the geometry of the molecule and its surroundings. In addition, as will be shown in Section 3.3, one ^{13}C site of the charged PE molecules gives rise to signals in this spectral range.

3.2.2 Lines a to j: Knight shifted lines

In Figure 5a the positions of all Knight shifted resonance lines *versus* temperature are given. In this graph the range of the position of the central line group is indicated by the broken lines (center of gravity given by open rhombs according to Fig. 4). The resonance lines a to j move towards the position of pure neutral perylene (marked by the thin solid line at 127.2 ppm) with decreasing temperature. These resonance lines are arranged in pairs: every two neighbouring lines keep their distance from each other. This is true for the lines g and h only above 220 K. Below this temperature they approach each other and merge below 180 K. Again, this is most likely due to the structural phase transition at $T_t = 213$ K.

According to equation (1) with a temperature independent isotropic hyperfine coupling constant a_i the Knight shifted lines have the same temperature behavior as the susceptibility of the conduction electrons $\chi_{ce}(T)$. Therefore, the line positions a to j are plotted in Figure 5b *versus* conduction electron susceptibility [2,3] with temperature as an implicit parameter. Evidently, the susceptibility of the conduction electrons describes the temperature behavior of the resonance positions very well. Therefore these resonance lines are unambiguously identified as Knight shifted lines originating from the perylene radicals of the conducting stacks.

3.2.3 Gated decoupling experiments

In these experiments there is a waiting period between the polarisation transfer and the observation of the carbon signal. During this evolution time the ^{13}C spins interact with the ^{1}H spins in a way that the spin polarization of the carbons is relaxing to that of the protons. By varying the evolution time we can detect the carbon positions which are directly bound to protons. For short evolution times, the resonance lines of carbons neighbouring a proton vanish because these have much shorter relaxation times than carbons with no proton neighbour.

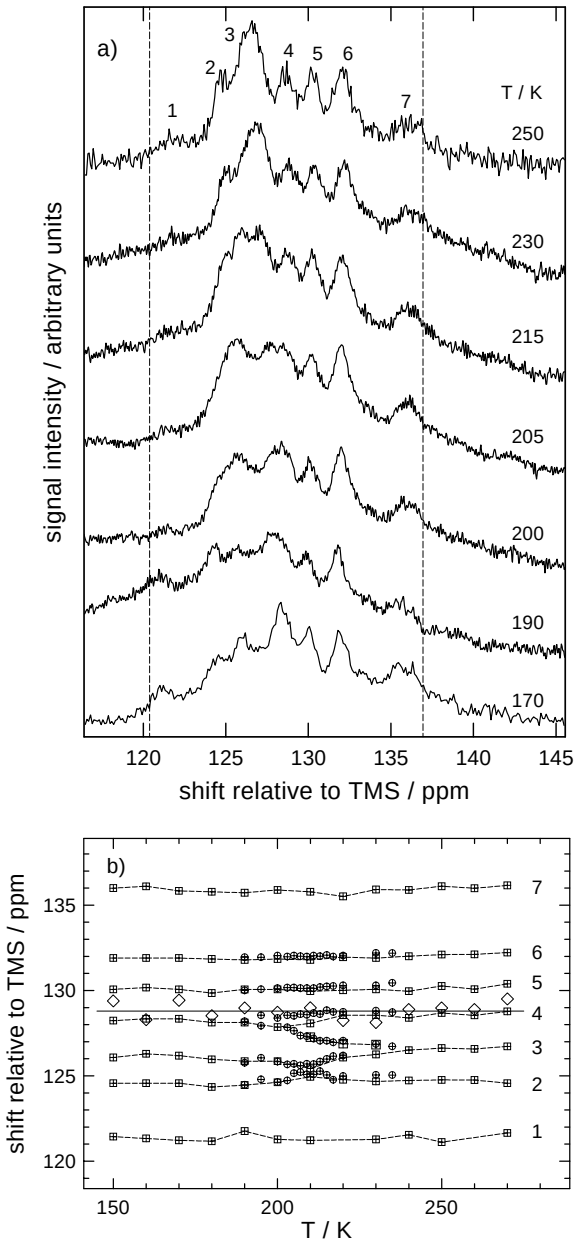

Fig. 4. (a) ^{13}C-CP-MAS spectra of the central line group of $(PE)_2PF_6 \cdot \frac{2}{3}THF$ at constant spinning frequency $f_{rot} = 3.7$ kHz. (b) Line positions *versus* temperature. The center of gravity of these lines is given by the open rhombs (the solid line indicates the mean value).

In order to characterise the lines a to j, at a constant temperature, $T = 220$ K, and spinning frequency (the latter depending on the peaks under examination) the evolution time τ was increased up to $\tau = 100$ μs. Again, two neighbouring resonance lines behave like pairs. After

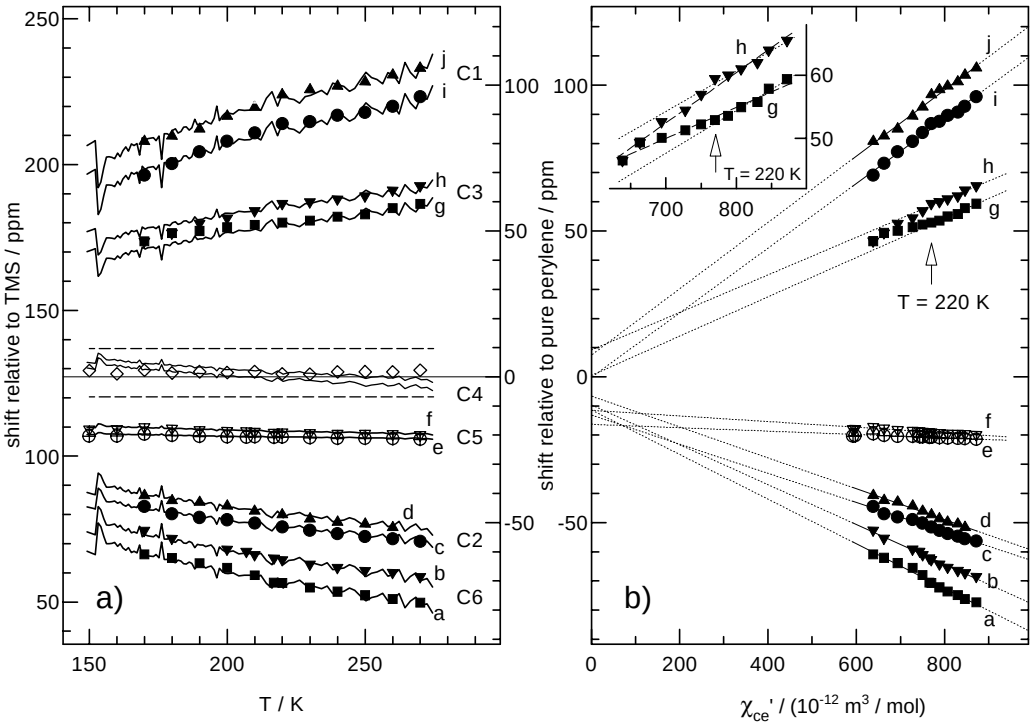

Fig. 5. Knight shifted lines from ^{13}C-CP-MAS spectra of $(PE)_2PF_6 \cdot \frac{2}{3}$THF. (a) Line positions *versus* temperature, (b) line positions *versus* susceptibility of the conduction electrons with temperature as an implicit parameter. For the solid lines and the labels see text.

long evolution times the lines c/d, g/h, and i/j have vanished. Therefore, they can be assigned to the protonated carbon position C1-C3 of the molecules in the conducting stack. On the other hand, the lines a/b and e/f are still visible under these conditions. Hence, they originate from carbon positions 4, 5 or 6 with no proton as a neighbour [9].

The evolution times used in the gated decoupling experiments for the lines of the central line group had much bigger values: they are still visible after an evolution time of $\tau = 1000\,\mu$s. Thus, by these experiments it would not be possible to distinguish the protonated from the other carbon positions for the neutral PE molecules in the RCS. These can only be the molecules which are perpendicular to the conducting stacks. The carbons on the wall molecules are polarised the same way as the carbons of the stack molecules, and both relax to the protons during the evolution time. But the protons in the stack have a much shorter relaxation time due to the contact interaction with the conduction electrons.

3.3 Derivation of local spin densities

By the purely experimental route, the lines c/d, g/h and i/j are thus identified as originating from the proton carrying carbons C1-C3 of intrastack perylene radicals. These are not the resonance signals of one type of PE stack molecule. The similarity in behavior of line pairs reveals that two inequivalent PE radicals are detected. This is in accordance to the inequivalence of two crystallographic sites of the highly symmetric perylene radicals occurring in the quasi-one dimensionally conductive stack. Any further association of NMR-lines and Knight shifts with carbon sites and molecular electronic spin densities requires an appropriate theoretical analysis based on MO calculations and empirical rules for hyperfine coupling constants. As in Section 3.1 for the neutral PE molecules, a three step approach was adopted (results in Tab. 2): based on *ab initio* MO calculations, a first approach for the spin density distribution on the PE radical was obtained [17]. With the help of the well-known Karplus-Fraenkel relation [18]

$$a_i = Q\rho_i + \sum_j Q_N \rho_j \qquad (2)$$

(with $Q = 99.7$ MHz of C1, C2, C3, $Q = 85.4$ MHz for C4, C5, C6 and $Q_N = -38.9$ MHz) the calculated ρ_i values were converted to a_i and K_i values. The latter by means of equation (1) and with the experimental $\chi_{ce}(T)$ values [2]. With the center of gravity of neutral perylene as reference, these K_i values allowed the identification of the carbon sites and the corresponding experimental shift values.

It is important to note, that by taking δ_i of the different carbon positions from the neutral perylene molecule the agreement between experimental and calculated K_i values is still unsatisfactory. This indicates that the different carbon positions of the perylene stack molecules have a different chemical shift than that of the neutral perylene molecule. Therefore, neutral perylene is given up as

Table 2. Comparison of calculated and experimental Knight shift, K_i, and spin density, ρ_i, values for the intrastack PE radicals in diperylene hexafluorophosphate and two other PE radical cation salts ($(PE)_2(AsF_6)_{0.75}(PF_6)_{0.35}\cdot 0.85CH_2Cl_2$ [15] and Au-dithiolate-PE [20]).

atom	$\rho_{i,\mathrm{cal}}$ [17]	$K_{i,\mathrm{cal}}$/ppm	$K_{i,\mathrm{exp}}$/ppm	$\rho_{i,\mathrm{exp}}$	$\rho_{i,\mathrm{cal}}$ [19]	$\rho_{i,\mathrm{cal}}$ [15]	$\rho_{i,\mathrm{exp}}$ [15]	$\rho_{i,\mathrm{cal}}$ [20]
C1	0.144	87.8	93.7/90.9	$0.189 \pm 0.001/0.192 \pm 0.003$	0.103	0.144	0.163	0.195
C2	−0.011	−57.8	−43.8/−41.7	$0.031 \pm 0.001/0.034 \pm 0.001$	0.012	−0.020	−0.020	−0.063
C3	0.097	44.8	55.3/52.8	$0.096 \pm 0.001/0.088 \pm 0.001$	0.087	0.107	0.173	0.150
C4	0.051	−4.5	–	$-0.046 \pm 0.001/-0.056 \pm 0.003$	0.046	0.041	0.013	−0.058
C5	−0.015	−22.7	−8.0/−4.8	$-0.053 \pm 0.001/-0.046 \pm 0.003$	0	−0.010	−0.055	0.203
C6	−0.029	−72.3	−63.6/−56.8	$0.012 \pm 0.001/0.034 \pm 0.001$	0	−0.032	−0.082	−0.074

a reference and the temperature behaviour of the measurement itself is employed: the experimental Knight shift values are taken from the Jaccarino-Clogston-plot (Fig. 5b). The extrapolation to zero electronic susceptibility gives the experimental reference for the Knight shift.

In Figure 5b every two resonance positions of a pair give parallel lines. For that reason, only values above 220 K -above the structural phase transition- are used for the extrapolation of the lines g and h to give their interception with the shift axis (see inset in Fig. 5b). The supposition of different chemical shifts δ_i of the carbon positions on the perylene radicals is supported by the fact that the interceptions with the shift axis do not agree with the δ_i of neutral perylene.

Then, for a fixed assignment of the carbon sites and experimental shifts K_i, agreement could be optimized by adjustment of the experimental values of the spin densities ρ_i and $\rho_{i'}$ of both inequivalent but approximately equally charged PE intrastack radicals [8]. Since one NMR line pair was not resolved, the normalization of $\sum_i \rho_i$ per radical was required as an additional restriction. The final results are given in Table 2 and reflected by the solid lines in Figure 5a. Evidently a reasonable fit to the observed line positions has been achieved.

In agreement with MO calculations [17,19] the carbon sites C1 and C3 carry the predominating spin densities. This was also observed in earlier studies of other perylene radicals [15,20]. The sensitivity of the calculated spin density distribution on the actual structural properties was exemplified already, in a comparison of isostructural substituted perylene[1] radical cation salts [21]. For the sites of the main spin densities, the differences in K_i or ρ_i between the two inequivalent PE radicals range below 10%, but outside the error bar. The extrapolation to zero conduction electron susceptibility and Knight shift in Figure 5b indicates that the chemical shifts, at corresponding sites of the two different PE molecules, differ most likely even to a larger extent. Nevertheless the center of gravity could almost be the same as indicated by the calculated shift values of carbon position 4.

[1] 1,2,7,8-tetrahydrodicyclopenta[cd, lm]perylene (CPP) and 3,4,9,10-tetramethylperylene (TMP).

4 Concluding remarks

^{13}C-CP-MAS high-resolution NMR proves the coexistence of charged paramagnetic and neutral diamagnetic perylene molecules in $(PE)_2PF_6 \cdot \frac{2}{3}THF$. The combination of X-ray structural analysis and *ab initio* molecular orbital calculations allows the correlation of the intramolecular bond length C4-C4* between the two naphthalene moieties of the perylene molecule and the average molecular charge [8]. Both sources of information unravel the correct description of the 2:1 stoichiometry in the perylene radical cation salt as $(PE)_4^{3+\bullet\bullet\bullet}(PE)_2^0(PF_6^-)_3\cdot 2THF$.

The detailed analysis of the NMR results explains the chemical shift data of the neutral PE molecules and the locally resolved Knight shift of the PE radicals. This is only attainable with the help of the temperature dependence of the conduction electron Pauli-paramagnetic susceptibility, appropriate *ab initio* MO calculations, and empirical relations for the hyperfine interaction. The NMR spectroscopic distinction of two different intra-stack PE radicals is in line with the crystallographic inequivalence of their structural sites. The careful analysis of the correlation between NMR-shift and electronic susceptibility, (K+δ)-*versus*-χ, reveals, that their chemical shift inequality may be more significant than the difference of their molecular electronic wave functions. Both are adding up to about 10% variation of the total shift at corresponding atomic sites. The C3-sites seem to be very susceptible to the H-F bonding between the PE stack molecules and the PF_6-anions. Thus, the chemical shift variation of the C3-sites, which is discovered at the monoclinic-triclinic phase transition, is in general agreement with structural and NMR-relaxation information [5,6].

Finally, it may be concluded that careful investigation of these supposedly simple radical cation salts explains their electronic and structural peculiarities in a consistent way.

We acknowledge discussions and contributions by R. Ahlrichs, C. Buschhaus, B. Pilawa, and M.H. Whangbo. We thank I. Odenwald for crystal growth. This work was supported by the Deutsche Forschungsgemeinschaft within the Sonderforschungsbereich 195 (Universität Karlsruhe (TH)).

References

1. H. Endres, H.J. Keller, B. Müller, D. Schweitzer, Acta Crystallogr. C **41**, 607 (1985).
2. M. Burggraf, H. Dragan, P. Gruner-Bauer, H.W. Helberg, W.F. Kuhs, G. Mattern, D. Müller, W. Wendl, A. Wolter, E. Dormann, Z. Phys. B **96**, 439 (1995).
3. A. Wolter, U. Fasol, R. Jäppelt, E. Dormann, Phys. Rev. B **54**, 12272 (1996).
4. U. Fasol, E. Dormann, Phys. Lett. A **222**, 281 (1996).
5. C. Buschhaus, E. Dormann, K. Eichhorn, K. Hümmer, R. Moret, S. Ravy, Synth. Met. **102**, 1757 (1999).
6. G. Nemec, V. Illich, E. Dormann, Synth. Met. **95**, 149 (1998).
7. G. Fischer, Ph.D. thesis, Universität Karlsruhe (TH), 1998.
8. G. Fischer, E. Dormann, Phys. Rev. B **58**, 7792 (1998).
9. G. Fischer, E. Dormann, Synth. Met. **103**, 2172 (1999).
10. P.C. Stein, P. Bernier, C. Lenoir, Phys. Rev. B **35**, 4389 (1987).
11. P.C. Stein, P. Bernier, Phys. Rev. B **37**, 10637 (1988).
12. S.J. Opella, M.H. Frey, J. Am. Chem. Soc. **101**, 5854 (1979).
13. D. Köngeter, M. Mehring, Phys. Rev. B **39**, 6361 (1989).
14. A. Sebald, MAS and CP-MAS of Less Common Spin-1/2 Nuclei, *NMR, Basic Principles & Progress*, edited by P. Diehl *et al.* (Berlin, 1994), Vol. 31.
15. J. Wieland, U. Haeberlen, D. Schweitzer, H.J. Keller, Synth. Met. **19**, 393 (1987).
16. M. Kollwitz, J. Gauss, Chem. Phys. Lett. **260**, 639 (1996).
17. J. Ziegler, B. Pilawa, Synth. Met. **82**, 53 (1996).
18. M. Karplus, G.K. Fraenkel, J. Chem. Phys. **35**, 1312 (1961).
19. D.K. Seo, M.H. Whangbo (unpublished results).
20. L. Firlej, A. Zahab, P. Bernier, Synth. Met. **70**, 1097 (1995).
21. P. Michel, A. Moradpour, P. Penven, L. Firlej, P. Bernier, B. Levy, S. Ravy, A. Zahab, J. Am. Chem. Soc. **112**, 8285 (1990).